distributions. Regularisation methods [1] were employed throughout the investigation and are based on a second-order derivative penalty function with the optimal regularisation parameter chosen by a generalized cross-validation technique. The various parameter distributions permit relatively small changes in composition and structure in one of the phases to be studied. For example, separation of a LAS-rich phase was detected on the surface of the drying mixture which effectively acted as a barrier to further drying. The spatially resolved moisture distributions for both test geometries are being used to verify and improve various droplet-drying models.

A fast pulsed field gradient (PFG) technique, Difftrain [2], which features a stimulated echo, was also used to measure the variation in apparent diffusion coefficient with Δ. These data enabled the tortuosity and surface-to-volume ratio of the water phase to be measured, as it resided amongst the solid constituent material. These measurements were performed as a function of moisture content within the mixture and as a function of drying rate. This was performed in situ on the same sample, as permitted by the rapid acquisition time of the Difftrain pulse sequence. Consequently, the evolving 'pore structure' occupied by the water was quantified during drying. These data are extremely useful in the generation of accurate models of the drying process, in particular the assignment of appropriate diffusion coefficients.

This work is supported by the EPSRC and an IMPACT Faraday Industrial CASE award with Proctor and Gamble.

[1] Wilson JD. J Mater Sci 1992:27:3911.
[2] Buckley C, Hollingsworth KG, Sederman AJ, Holland DJ, Johns ML, Gladden LF. J Magn Reson 2003;161:112.

doi:10.1016/j.mri.2007.01.045

NMR of diffusion in porous media: branched or disordered structure?

D.S. Grebenkov[a], *G. Guillot*[b]
[a]*Dipart di Scienze Fisiche, Univ Napoli, Italy,* [b]*U2R2M, CNRS-Univ Paris-Sud UMR8081, 91405 Orsay, France*

Measurement of the spin-echo attenuation due to restricted diffusion is a usual NMR technique to probe the geometry of porous media [1]. In particular, the surface-to-volume ratio of statistically isotropic confining domain could be found in the slow diffusion regime [2]. However, natural morphologies often exhibit a complex internal architecture (e.g., branching of the pulmonary acinus or pore network in rocks). One may thus wonder what is the role of such structures for NMR measurements?

To answer these questions, we have performed Monte Carlo simulations of restricted diffusion in three groups of three-dimensional structures with the same surface-to-volume ratio (Fig. 1). A basic domain was a cube of size L divided into 216 small cubic cells. The first group (A) was a set of random dichotomic labyrinths generated inside the cube by the Kitaoka algorithm [3]. The second group (B) consisted of two realizations of a long channel filling the same cube. In the third group (C), disordered porous media were generated by connecting a number of randomly chosen adjacent cells.

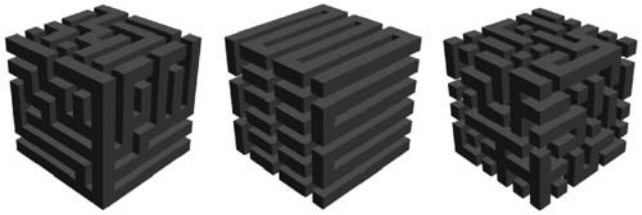

Fig. 1. Different porous media with an identical surface-to-volume ratio: a Kitaoka labyrinth (A), a long channel (B) and a disordered structure (C).

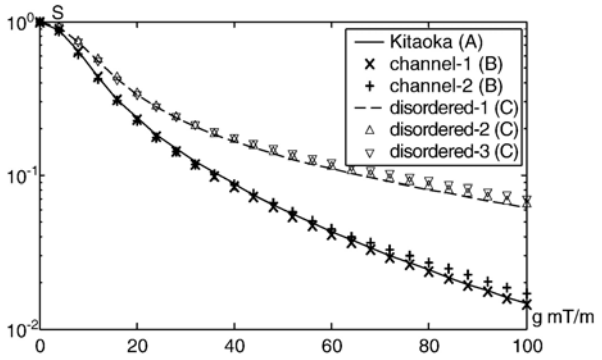

Fig. 2. Signal $S_{av}(g)$ for different porous structures shown in Fig. 1.

Stochastic trajectories of the diffusive motion $\mathbf{r}(t)$ with normal reflections on the boundary have been modeled as a sequence of n independent normally distributed random jumps with dispersion $(2D\tau)^{1/2}$, where D was the free diffusion coefficient, $\tau = T/n$ the smallest time scale and T the echo time. The total dephasing accumulated by a diffusing spin in a steady linear magnetic field gradient of intensity g in direction $\mathbf{e}$ was calculated as $(\mathbf{e}_x\varphi_x+\mathbf{e}_y\varphi_y+\mathbf{e}_z\varphi_z)$, where dephasing φ_i in direction i was

$$\varphi_i = \gamma g t \mathbf{e} \cdot \left(\sum_{k=1}^{n/2} \mathbf{r}(k\tau) - \sum_{k=n/2}^{n} \mathbf{r}(k\tau) \right)$$

γ being the nuclear gyromagnetic ratio (the minus sign accounts for gradient inversion, from the 180° RF pulse). The direction $\mathbf{e}$ of the applied gradient was uniformly averaged over all spatial orientations to reproduce isotropic behavior. The signal $S_{av}(g)$ was then obtained as the expectation:

$$S_{av}(g) = (4\pi)^{-1} \int_{|e|=1} d\mathbf{e} \boldsymbol{E}\{exp[i(\mathbf{e}_x\varphi_x + \mathbf{e}_y\varphi_y + \mathbf{e}_z\varphi_z)]\} = \boldsymbol{E}\{sin(\varphi)/\varphi\}$$

where $\varphi = (\varphi_x^2+\varphi_y^2+\varphi_z^2)^{1/2}$. The probability distribution of the random variable $\ddot{u}$ was obtained by repeating Monte Carlo simulations N times. For water diffusion ($\gamma = 2.675 \cdot 10^8$ rad T^{-1} s^{-1}, $D = 2.3 \cdot 10^{-9}$ m^2/s) in a porous medium ($L = 60$ μm) with $T = 150$ ms, numerical results are summarized in Fig. 2 (here we used $N = 10^6$ and $n = 10^3$). One can see that the signal attenuation $S_{av}(g)$ for different *branched* structures (Groups A and B) are almost identical, while the signal for *disordered* media (Group C) is significantly higher. This is related to the fact that a disordered medium consists of a number of small disconnected patterns where the signal is less attenuated. We conclude that the internal structure of porous media may influence the restricted diffusion and NMR measurements and should be taken into account for practical applications.

[1] Callaghan PT, et al. Nature 1991;351:467.
[2] Mitra PP, et al. Phys Rev Lett 1992;68:3555.
[3] Kitaoka H, et al. J Appl Physiol 2000;88:2260.

doi:10.1016/j.mri.2007.01.046

Probing a model pulmonary acinus by NMR gas diffusion

D. Habib[a], *D. Grebenkov*[a,b], *G. Guillot*[a]
[a]*CNRS-Univ Paris-Sud UMR8081 Orsay France,* [b]*Dipartimento di Scienze Fisiche, Univ Napoli Italy*

Pathological changes in human lungs due to emphysema have been observed using MRI with hyperpolarised helium-3 (HP-^{3}He) [1,2]. The

behavior of signal attenuation as a function of gradient intensity G is generally analyzed with a simple Gaussian model. But the 3D architecture of the pulmonary acinus is a dichotomic branching structure, which could cause deviation from the Gaussian behavior. We performed measurements of HP-^{3}He NMR signal attenuation with a bipolar gradient pulse on a 3D phantom (cube of 28 mm internal size, with channels of 3 mm square section) made by stereolithography with a branching architecture following Kitaoka's algorithm [3]. Different pressures and gas compositions were examined, thus covering for the free diffusion coefficient the range D_0=0.4–28 cm^2/s, keeping identical timing for the bipolar gradient pulse (total duration T=10 ms). The signal attenuation as a function of G was fitted to a Gaussian model with a single apparent diffusion coefficient (ADC) and also compared to results from Monte Carlo simulations of the reflected Brownian motion.

Signal amplitude was determined within better than 0.1%. Fig. 1 shows signal attenuation as a function of G for the smaller and larger D_0's explored. The Gaussian model gave a reasonable estimate of experimental results at low G, but poorer at lower pressures, while numerical results showed the best agreement to experiments on the whole G range whatever D_0. Fig. 2 shows $(1-\mathrm{ADC}/D_0)$ plotted against the diffusion length $(D_0T)^{1/2}$, for G along the three orientations. At small D_0T, all data collapsed onto a single curve, as expected for the ADC/D_0 dependence on diffusion length [4] and giving similar surface-to-volume ratio along each direction (4.44 cm^{-1}), when the exact gradient timing was taken into account [5].

[1] Saam et al. Magn Reson Med 2000;44:174–9.
[2] Swift et al. European J Radiol 2005;54:352–8.
[3] Kitaoka et al. J Appl Physiol 2000;88:2260–8.
[4] Mair et al. Phys Rev Lett 1999;83:3324–7.
[5] Grebenkov. 2006 [submitted].

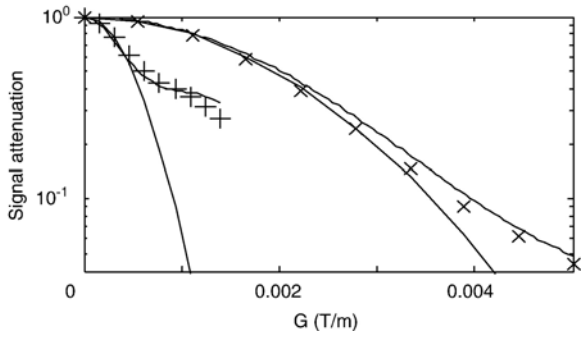

Fig. 1. HP-3He NMR signal as a function of G for 3He at 70 hPa (+), and for a nitrogen-3He mixture at 2000 hPa (×), best fits to Gaussian model (dashed lines) and results from Monte Carlo simulations (full lines).

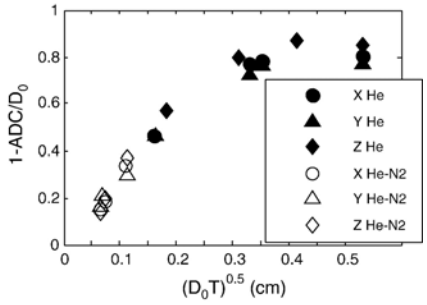

Fig. 2. (1−ADC/D0) plotted against the diffusion length $(D_0T)^{1/2}$.

doi:10.1016/j.mri.2007.01.047

Volume flow rate distribution in flow (non-Newtonian) through porous bone structure

C. Heinen[a], *T. Zeiser*[b], *G. Baroud*[a]
[a]*Department of mechanical Engineering, University of Sherbrooke, Quebec, Canada,* [b]*University of Erlangen-Nuremberg, Germany*

Background: One complication during the vertebroplasty process (filling the osteoporotic vertebra by injection of a curing two-component bone cement to re-stabilize the spine) is leakage, the uncontrolled flow of cement out of the vertebra into the environment. Leakage may lead to serious postoperative problems for the treated person and can even lead to death. To find and prevent this kind of complication at an early stage of the application process, it is desirable to find and prevent main flow paths in the bone while injecting the cement. Ideally, the cement flows from the outlet of the cannula uniformly in all directions, ignoring the few obstacles built from the osteoporotic bone structure (porosity up to 95%). This ideal behavior of the cement is determined, e.g., by the time delay from mixing to injection and from the injection rate. The final intention is the online monitoring and control of the flow patterns of the cement by MRI. This paper contributes to the determination of the volume flow rate distribution as to finding main flow paths out of MRI velocity data.

Method: The picture on the left shows schematically the projection of a 2D spatially resolved velocity profile in a cross section of bone structure. If Q, the volume flow rate with velocities, is greater than the threshold $w_s/\bar{w}$ ($\bar{w}$, mean velocity) and A_{eff}, the total part of the cross-section area used from Q, then a volume flow rate distribution P can be calculated by variation of the threshold. If $A_{\mathrm{eff}}(Q/Q_{\mathrm{ent}})$ is normalized by A_{ent}, the entire cross section of flow, one can get an effective porosity of the structure depending on Q/Q_{ent}. P indicates the part of the cross-section area that carries velocities greater than the threshold (cf. Buggisch).

Results: The picture on the right side shows the approximate calculated volume flow rate distribution of a low Reynolds number Newtonian fluid channel flow through an ostoeporotic bone structure (CT data). These results are obtained from a simulated flow study that uses the lattice-Boltzmann method, which was first tested on flow through bead packing [1]. This picture is color coded: blue — areas of low velocities, green — areas of medium velocities, and yellow — areas of high velocities.

Discussion: The Newtonian simulation shows that the flow is controlled by the cavities of the bone structure and that the flow pattern is nonuniform. Previous performed leakage experiments of bone cement flow (non-Newtonian, viscoelastic, time dependant) through Al-foam bone substitutes (equal porosity) demonstrate the possibility of acquiring uniform flow pattern using the bone cement. Hereafter, the project will be focused on the demonstration of the physical and rheological properties of the cement and on the geometric properties of the bone cavities.